









RESEARCH ARTICLE | DECEMBER 08 2023

# Reducing proton radiation vulnerability in AlGaN/GaN high electron mobility transistors with residual strain relief

Nahid Sultan Al-Mamun  ; Joonyup Bae  ; Jihyun Kim  ; Aman Haque   ; Douglas E. Wolfe  ; Fan Ren  ; Stephen J. Pearton 

 Check for updates

*J. Appl. Phys.* 134, 224901 (2023)

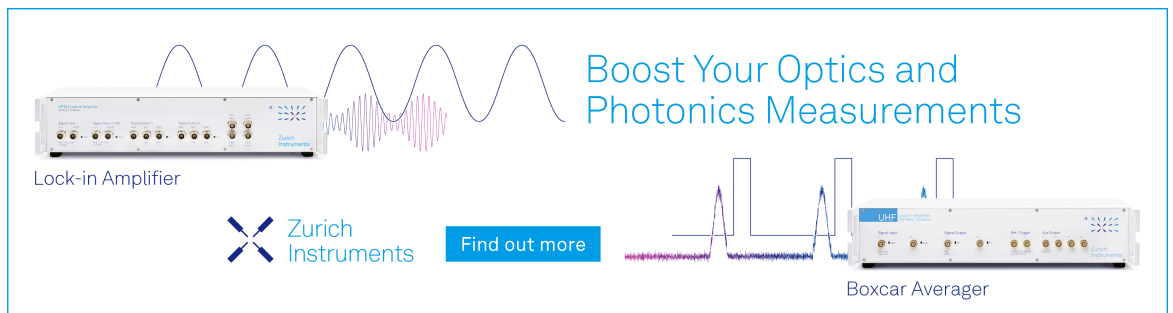
<https://doi.org/10.1063/5.0169886>



View Online




Export Citation



Boost Your Optics and Photonics Measurements

Lock-in Amplifier

 Zurich Instruments

[Find out more](#)

Boxcar Averager

# Reducing proton radiation vulnerability in AlGaIn/GaN high electron mobility transistors with residual strain relief

Cite as: J. Appl. Phys. 134, 224901 (2023); doi: 10.1063/5.0169886

Submitted: 29 July 2023 · Accepted: 19 November 2023 ·

Published Online: 8 December 2023



Nahid Sultan Al-Mamun,<sup>1</sup> Joonyup Bae,<sup>2</sup> Jihyun Kim,<sup>2</sup> Aman Haque,<sup>1,a)</sup> Douglas E. Wolfe,<sup>3</sup>   
Fan Ren,<sup>4</sup> and Stephen J. Pearton<sup>5</sup>

## AFFILIATIONS

<sup>1</sup>Department of Mechanical Engineering, Penn State University, University Park, Pennsylvania 16802, USA

<sup>2</sup>School of Chemical and Biological Engineering, Seoul National University, Gwanak-gu, Seoul 08229, Republic of Korea

<sup>3</sup>Department of Materials Science and Engineering, Penn State University, University Park, Pennsylvania 16802, USA

<sup>4</sup>Department of Chemical Engineering, University of Florida, Gainesville, Florida 32611, USA

<sup>5</sup>Department of Material Science and Engineering, University of Florida, Gainesville, Florida 32611, USA

<sup>a)</sup>Author to whom correspondence should be addressed: mah37@psu.edu

## ABSTRACT

Strain plays an important role in the performance and reliability of AlGaIn/GaN high electron mobility transistors (HEMTs). However, the impact of strain on the performance of proton irradiated GaN HEMTs is yet unknown. In this study, we investigated the effects of strain relaxation on the properties of proton irradiated AlGaIn/GaN HEMTs. Controlled strain relief is achieved locally using the substrate micro-trench technique. The strain relieved devices experienced a relatively smaller increase of strain after 5 MeV proton irradiation at a fluence of  $5 \times 10^{14} \text{ cm}^{-2}$  compared to the non-strain relieved devices, i.e., the pristine devices. After proton irradiation, both pristine and strain relieved devices demonstrate a reduction of drain saturation current ( $I_{ds,sat}$ ), maximum transconductance ( $G_m$ ), carrier density ( $n_s$ ), and mobility ( $\mu_n$ ). Depending on the bias conditions the pristine devices exhibit up to 32% reduction of  $I_{ds,sat}$ , 38% reduction of  $G_m$ , 15% reduction of  $n_s$ , and 48% reduction of  $\mu_n$  values. In contrast, the strain relieved devices show only up to 13% reduction of  $I_{ds,sat}$ , 11% reduction of  $G_m$ , 9% reduction of  $n_s$ , and 30% reduction of  $\mu_n$  values. In addition, the locally strain relieved devices show smaller positive shift of threshold voltage compared to the pristine devices after proton irradiation. The less detrimental impact of proton irradiation on the transport properties of strain relieved devices could be attributed to reduced point defect density producing lower trap center densities, and evolution of lower operation related stresses due to lower initial residual strain.

Published under an exclusive license by AIP Publishing. <https://doi.org/10.1063/5.0169886>

## INTRODUCTION

Gallium nitride (GaN) is one of the most attractive wide-bandgap semiconductor materials for next generation electronics requiring high power, high frequency, high speed, and high temperature due to its excellent electrical, thermal, and optical properties.<sup>1,2</sup> The superior performance of GaN-based devices is the result of the large bandgap, high critical electric field, high electron saturation velocity and mobility, and good thermal conductivity.<sup>3,4</sup> One of the most promising GaN-based devices is the AlGaIn/GaN high electron mobility transistor (HEMT), where the spontaneous and piezoelectric polarizations of GaN are utilized to form a

two-dimensional electron gas (2DEG) at the AlGaIn/GaN hetero-interface providing high electron mobility and very low specific ON-resistance without any intentional doping.<sup>5,6</sup> Besides excellent electrical transport properties, the GaN-based devices demonstrate very good radiation tolerance due to the high displacement threshold energy of GaN resulting from its small lattice constants.<sup>7-9</sup> The GaN devices also show good ionization resistance and self-healing phenomena at room temperature.<sup>10,11</sup> The AlGaIn/GaN HEMTs provide additional radiation hardness due to the very small cross section of the 2DEG channel, which modulates the transport properties of the device. As a result, GaN-based devices are very

07 April 2024 10:49:38

attractive for harsh radiation environment applications such as space exploration, satellite-based wireless communications, radar, defense electronics, and nuclear power plants.<sup>12</sup>

Electronic devices are susceptible to radiation induced degradation in harsh environments due to repeated exposure of high energy photons such as gamma and x rays, neutrons, and charged particles such as protons and alpha particles.<sup>8,11</sup> The energetic particles and photons degrade the device's performance through ionization and displacement damage. GaN-based devices also experience radiation induced degradation to some extent.<sup>4,7,8,11</sup> Extensive research has been reported in the literature on the proton irradiation effects on the transport properties of AlGaIn/GaN HEMTs.<sup>13–27</sup> Studies have been performed on wide range of proton energy ranging from 100 keV to 105 MeV<sup>18,26</sup> and fluence values ranging from  $1 \times 10^{10}$  to  $2 \times 10^{16}$  protons/cm<sup>2</sup>.<sup>18,19</sup> Noticeable degradation of GaN HEMTs is usually observed with proton energy greater than 2 MeV with fluence of  $>1 \times 10^{14}$  protons/cm<sup>2</sup>.<sup>8</sup> In general, at a fixed proton energy, the higher fluence level induces higher degradation of GaN HEMTs, whereas, at the fixed fluence level, lower proton energy shows more detrimental effect of GaN HEMTs. Lower energies produce larger non-ionizing energy loss (NIEL) within the 2DEG, resulting in a higher probability of defect generation. As a result, a higher number of defects are generated in the AlGaIn barrier layer and the GaN buffer layer and/or the AlGaIn/GaN interface, where the 2DEG layer is located. However, all of the proton irradiation studies of GaN HEMTs are primarily focused on the degradation of device performance relating to the type of defects and defect generation mechanisms as a function of different combinations of proton energy and fluence,<sup>13,18,20,26–28</sup> device heterostructures, substrates, and fabrication scheme.<sup>14,29–34</sup>

The unique heterostructure of AlGaIn/GaN HEMTs inevitably introduces strain within the device layers, which originates from the mismatch of lattice constants and thermal expansion coefficients of active device layers and the substrate materials.<sup>35,36</sup> The study of strain effects on the performance of AlGaIn/GaN HEMTs has achieved a lot of attention due to the strain dependency of 2DEG transport properties.<sup>37–40</sup> The combined effect of strain in the interfacial layers of 2DEG, i.e., the GaN, which could be under tensile or compressive strain depending on the substrate, and the AlGaIn, which is mostly under tensile strain,<sup>11,41</sup> determines the overall strain status of the 2DEG. It has been reported that tensile strain increases the 2DEG conductivity by increasing the carrier density and mobility.<sup>37,42,43</sup> However, the existing strain literature of GaN HEMTs is mostly concerned with uniform strain achieved by mechanical bending,<sup>39,40</sup> cantilever structures,<sup>37</sup> different substrate materials,<sup>36</sup> and partial removal of the substrate.<sup>43,44</sup> But non-uniform strain or localized strain distribution is very prevalent in electronic devices arising from different device features such as contact pads, passivation layers, field plates, non-uniformity of the substrate itself, and process related non-uniformity. The impact of localized strain distribution along and across the device channel is mostly neglected due to the very small global average of localized strain, which apparently has an inconsequential response to the global transport properties of the device. The difficulty of controlling strain locally and the difficulty in accurate measurement of strain within a very small, confined region is also an impediment to study localized strain effects. Therefore, only a handful of research

is available on the localized strain distribution effect on the performance and reliability of GaN HEMTs.<sup>45–47</sup>

The motivation for this research arises from the strain dependent performance of AlGaIn/GaN HEMTs. The strain effects and proton irradiation effects on the performance of GaN HEMTs have been separately reported in the literature. However, no experimental study has been performed yet on the impact of strain on the proton irradiated GaN HEMTs, let alone localized strain. Using atomic scale simulations in combination with the Monte Carlo method and the carrier transport theory, Li *et al.*<sup>48</sup> recently have reported that compressive strain can enhance the proton irradiation tolerance of GaN HEMTs by reducing defect density, whereas the tensile strain can degrade the proton irradiation hardness. Therefore, it is important to experimentally investigate the synergistic effect of strain and proton irradiation in GaN HEMTs. In this research, we investigated the proton irradiation effect on the transport properties of localized strain relieved AlGaIn/GaN HEMTs.

## EXPERIMENTAL DETAILS

Commercially available depletion mode AlGaIn/GaN HEMT dies (CGHV60008D, Wolfspeed<sup>®</sup>) on SiC substrates were used in this research. For localized strain relaxation, we employed the substrate micro-trenching technique by focused ion beam (FIB), a widely used method for controlled residual stress relief and measurement.<sup>49,50</sup> A 70  $\mu\text{m}$  deep trench of  $20 \times 30 \mu\text{m}^2$  size was milled on the 100  $\mu\text{m}$  substrate under each device channel of the six-fingered device using FEI Scios two dual beam FIB equipped with gallium ion ( $\text{Ga}^+$ ) source. The details of strain relaxation by the substrate micro-trenching can be found in Ref. 51. The cross-sectional schematics of a single channel of the pristine and micro-trenched devices are shown in Fig. 1.

Proton irradiations were performed at the Korean Institute of Radiological and Medical Sciences using an MC 50 (Scanditronix) cyclotron. The proton energy was held constant at 5 MeV. The irradiated fluence was  $5 \times 10^{14} \text{ cm}^{-2}$  at a constant beam current of 10 nA. The irradiation time was 5089 s.

Micro-Raman spectroscopy was used to measure the strain in the GaN layer of the devices using a Horiba LabRAM HR Evolution coupled with 100 $\times$ , NA=0.9 microscope objective. The high-resolution Raman spectra were obtained using a 532 nm (Oxxious LCX-Nd:YAG) green laser with an incident power <4 mW, a confocal hole/slit set to 50  $\mu\text{m}$ , an 1800 g/mm grating, and a Si array back illuminated deep depleted detector (Horiba-Synapse). The Raman maps were recorded with 2 and 0.5  $\mu\text{m}$  step intervals along and across the device channel, respectively. The position and full width at half maximum (FWHM) of the peaks were extracted after fitting the Raman spectra using the Pseudo-Voigt peak fitting model. All electrical characterization was performed at room temperature on a Cascade 1200 probe station equipped with a Keithley 4200A-SCS semiconductor parameter analyzer.

## RESULTS AND DISCUSSIONS

Stopping and Range of Ions in Matter (SRIM)<sup>52,53</sup> simulation was performed to obtain the energy loss of 5 MeV proton in the AlGaIn/GaN heterostructure and irradiation induced vacancy distribution. The simulated total energy loss, i.e., the electronic energy

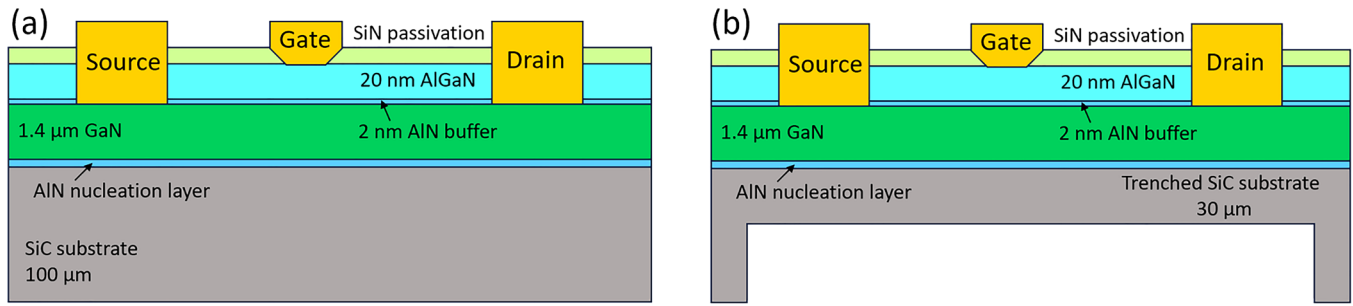


FIG. 1. Cross-sectional schematics of (a) pristine and (b) micro-trenched ( $20 \times 30 \mu\text{m}^2$ ) (along the plane of trenching, not drawn up to scale) devices.

loss and nuclear energy loss, as a function of projected penetration depth is shown in Fig. 2(a). The projected range of 5 MeV protons is higher than  $200 \mu\text{m}$ , which suggests most of the ions pass through the  $\sim 102 \mu\text{m}$  AlGaN/GaN HEMT structure including the SiC substrate. The active device layers, i.e., the AlGaN and GaN layers, are located at a shallow penetration depth, below  $0.3 \mu\text{m}$  thick SiN passivation layer. As a result, the energy loss in the active device layers is primarily by electronic stopping causing ionization. Most of the nuclear energy loss is deposited into the SiC below the HEMT structure. However, the high energy proton ions interact with the Schottky and Ohmic contacts of the device containing heavy elements such as gold and platinum. As a result, the bombarded proton ions scatter with lower energy into the 2DEG interface region creating vacancies and a cascade of defects by non-ionizing energy loss (NIEL). The distribution of gallium and

nitrogen vacancies in the AlGaN and GaN layers as a function of penetration depth of 5 MeV proton ions is shown in Fig. 2(b). The density of gallium vacancies is found to be relatively higher compared to nitrogen vacancies due to the higher displacement energy of nitrogen.<sup>13</sup> Gallium vacancies act as acceptor like defects and nitrogen vacancies act as donor like defects. These defects are responsible for the degradation of 2DEG carrier density and mobility.<sup>9,28,54–56</sup>

The in-plane strain ( $\epsilon_{xx}$ ) in the GaN HEMTs was obtained by high-resolution micro-Raman spectroscopy. The  $\epsilon_{xx}$  value was estimated using the frequency shift of the GaN  $E_2$  (high) phonon mode compared to the strain free  $E_2$  (high) phonon frequency.<sup>36,57,58</sup> The in-plane strain distribution before proton irradiation of the pristine and micro-trenched devices is shown in Fig. 3(a). The in-plane tensile strain values of the pristine devices

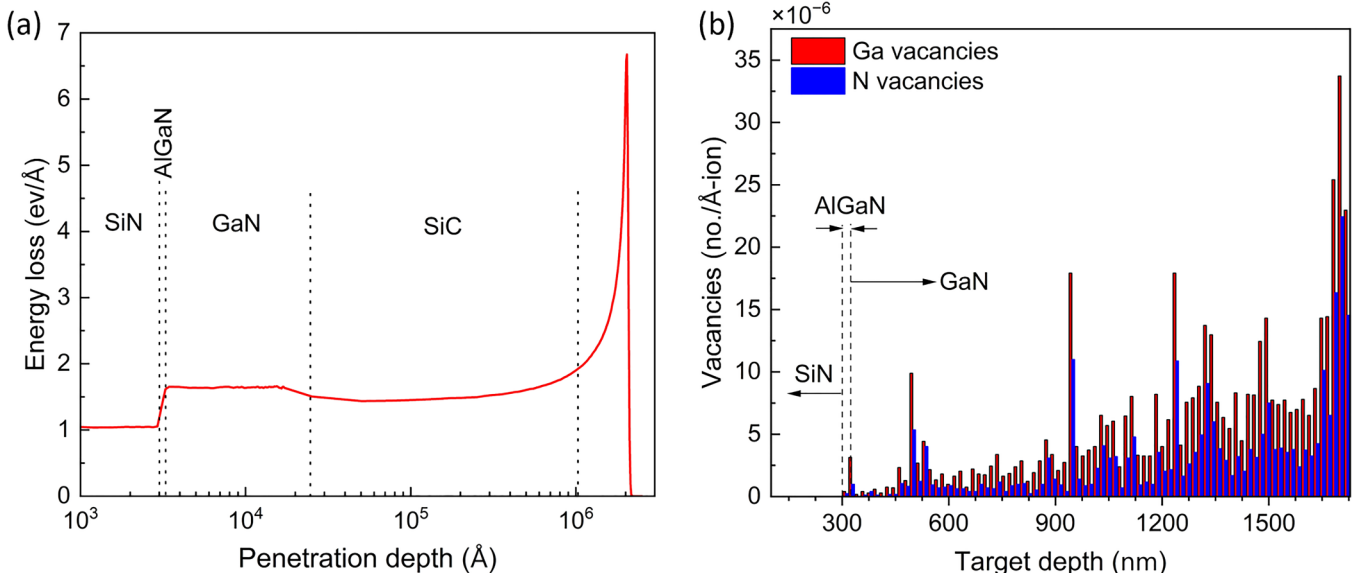
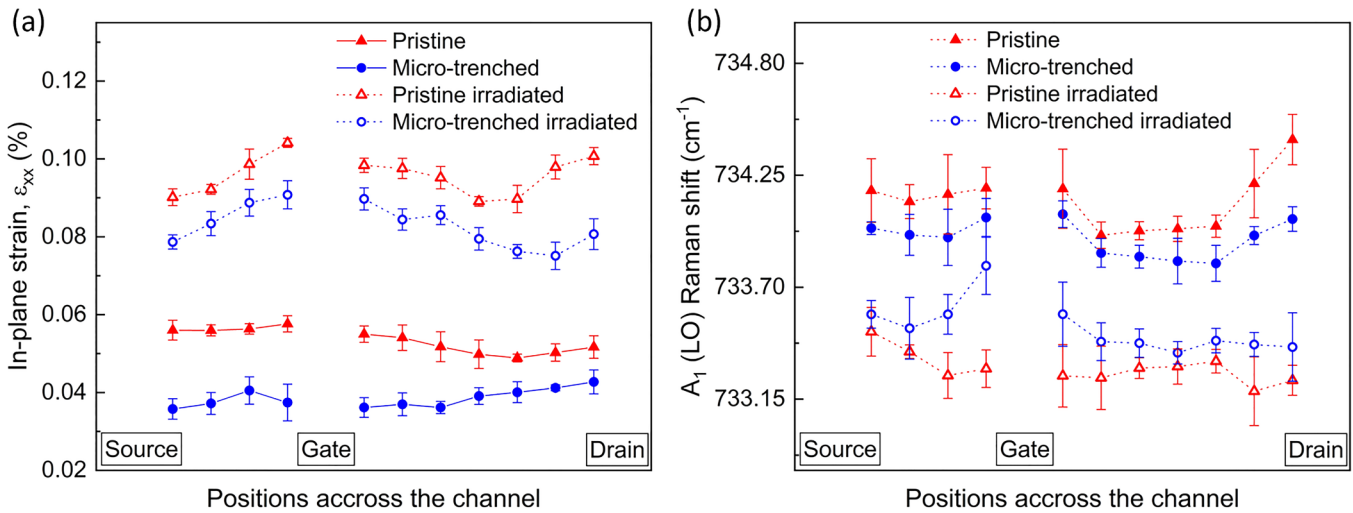


FIG. 2. SRIM simulation results showing (a) total energy loss and (b) gallium and nitrogen vacancy distribution by 5 MeV proton as a function of penetration depth into the AlGaN/GaN heterostructure.

07 April 2024 10:49:38



**FIG. 3.** Micro-Raman results across the device channel showing (a) in-plane strain distribution and (b)  $A_1$  (LO) phonon peak position of the pristine and micro-trenched devices (at the location of strain relief) before and after proton irradiation.

vary from  $0.049 \pm 0.001\%$  to  $0.057 \pm 0.002\%$  across the channel from source to drain regions. The micro-trenched devices demonstrate a relaxation of tensile strain at the vicinity of the trench because of partial removal of the substrate, and the corresponding  $\epsilon_{xx}$  values vary from  $0.036 \pm 0.002\%$  to  $0.042 \pm 0.003\%$ . After proton irradiation, the in-plane strain of both devices increases. The  $\epsilon_{xx}$  values of the pristine and micro-trenched devices are found to vary from  $0.089 \pm 0.003\%$  to  $0.1 \pm 0.002\%$  and  $0.075 \pm 0.003\%$  to  $0.091 \pm 0.003\%$ , respectively. The post-irradiation strain distribution reveals the presence of higher strain at the gate and drain edges of the channel for both devices. The initial higher values of the strain of the pristine devices led to post-irradiation higher strain distribution compared to the micro-trenched devices. We observed approximately 0.3–0.4 and 0.5–0.6  $\text{cm}^{-1}$  red shift of the SiC substrate TO and LO phonon modes, respectively. This red shift of SiC Raman peaks represents the increase of the strain level of the SiC substrate itself, which can translate into the GaN layer increasing its strain. However, several studies in the literature, involving the sapphire substrate, observed no change in the post-irradiation strain in GaN.<sup>59–61</sup> Such a discrepancy could be attributed to the difference in the initial strain/defect level, substrate materials, irradiation energy, and fluence. To study the contribution of different materials, we performed SRIM simulation of SiC and sapphire substrates, keeping all other parameters the same. The penetration depth and energy loss for SiC were found to be  $200 \mu\text{m}$  and  $6.5 \text{ eV}/\text{\AA}$ , respectively [Fig. 2(a)]. Corresponding values for sapphire were  $240 \mu\text{m}$  and  $5.5 \text{ eV}/\text{\AA}$ . We suggest that the higher stopping power of SiC could explain why we observed higher post-irradiation strain compared to the studies using sapphire.

The frequency distribution of the GaN  $A_1$  (LO) Raman peak before and after irradiation is shown in Fig. 3(b). The frequency of the  $A_1$  (LO) peak of the pristine devices is found to be higher compared to the micro-trenched devices before proton irradiation,

suggesting higher free carrier concentration of the pristine devices according to the theory of coupled plasmon  $A_1$  (LO) phonon mode.<sup>62,63</sup> After irradiation, the  $A_1$  (LO) phonon frequency of both devices shifts toward a lower wavenumber indicating the reduction of free carrier concentration due to proton irradiation. However, intriguingly, the  $A_1$  (LO) phonon frequency of the micro-trenched devices at the trench location is found to be relatively higher compared to the pristine devices after irradiation, which implies that the reduction of free carrier concentration due to proton irradiation in the micro-trenched region is less severe compared to the pristine counterpart. After proton irradiation, the FWHM values of the  $E_2$  (high) and  $A_1$  (LO) peaks for the pristine devices increase from  $2.52 \pm 0.1$  to  $2.97 \pm 0.14$  and  $6.17 \pm 0.18$ – $6.91 \pm 0.12 \text{ cm}^{-1}$ , respectively. In the case of the micro-trenched devices, the FWHM values of the  $E_2$  (high) and  $A_1$  (LO) peaks increase from  $2.63 \pm 0.06$  to  $2.95 \pm 0.11$  and  $6.26 \pm 0.15$ – $6.69 \pm 0.09 \text{ cm}^{-1}$ , respectively. The broadening of Raman peaks after proton irradiation indicates the increased defect density in the GaN layer, which could contribute to the degradation of electrical properties by increasing the trap density in the device. The slightly narrower  $A_1$  (LO) peak of the irradiated micro-trenched devices compared to the irradiated pristine devices suggests relatively lower defect density, which could reduce the proton irradiation induced degradation of electrical properties of the micro-trenched devices.

The output characteristic curves ( $I_{ds}$ – $V_{ds}$ ) and the transfer curves ( $I_{ds}$ – $V_{gs}$ ) of the pristine and micro-trenched devices before proton irradiation are shown in Figs. 4(a) and 4(b), respectively. The micro-trenched devices show higher ON-resistance ( $R_{ON}$ ), which is the reciprocal of the slope of  $I_{ds}$ – $V_{ds}$  curves, compared to the pristine devices. The ON-resistances of the pristine and micro-trenched devices are calculated to be 3.7 and 4.28  $\Omega$ , respectively, at zero gate voltage ( $V_{gs} = 0 \text{ V}$ ). The saturation drain current ( $I_{ds,sat}$ ) of the micro-trenched devices is also found to be smaller compared



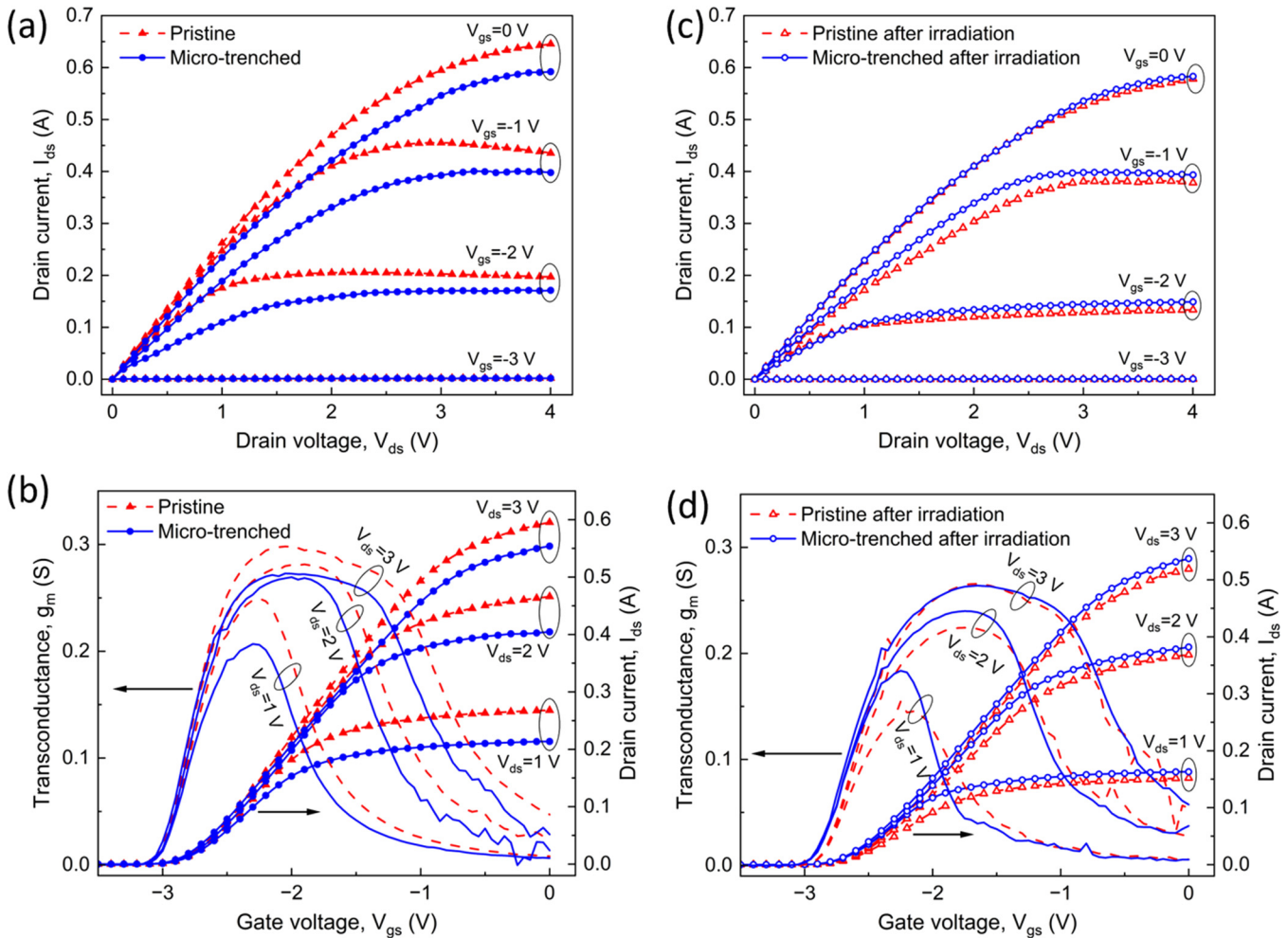


**FIG. 4.** Transport characteristics of the pristine and micro-trenched devices showing (a) output curves and (b) transfer curves before radiation, and (c) output curves and (d) transfer curves after radiation.

to the pristine devices. The higher  $R_{ON}$  and smaller  $I_{ds,sat}$  of the micro-trenched devices is the result of partial relief of in-plane strain in the GaN layer, as shown in Fig. 3(a), at the middle of each channel of the six-channel device. The partial relaxation of the strain also reduces the transconductance of the devices, as shown in Fig. 4(b). However, such partial relaxation of strain does not change the threshold voltage ( $V_{th}$ ) of the devices, which is found to be  $-3$  V for both devices. The output characteristics and the transfer curves of the devices after proton irradiation are presented in Figs. 4(c) and 4(d), respectively. Noticeable increases of  $R_{ON}$  and reduction  $I_{ds,sat}$  are observed for both devices after irradiation. Both of the devices experience a positive shift of threshold voltage, which results from negatively charged traps in the AlGaIn barrier layer and/or the GaN buffer layer.<sup>11</sup> The threshold voltage of the pristine and micro-trenched device shifts to  $-2.85$  and  $-2.92$  V, respectively. The maximum transconductance ( $G_M$ ) of the devices

also decreased after proton irradiation. Proton irradiation displaces atoms from the AlGaIn and GaN layer creating nitrogen interstitials and gallium–nitrogen divacancies. These defects act as acceptor like traps in the AlGaIn/GaN 2DEG interface causing a positive shift of threshold voltage and reduction of transconductance.<sup>11,64</sup>

The relative change of drain saturation current ( $\Delta I_{ds,sat}$ ), ON-resistance ( $\Delta R_{ON}$ ), and maximum transconductance ( $\Delta G_M$ ) for different gate and drain bias conditions of the pristine and localized strain relieved devices are represented in Figs. 5(a) and 5(b). The reduction of  $I_{ds,sat}$  and increase of  $R_{ON}$  values of the pristine devices are relatively larger compared to the micro-trenched devices, as shown in Fig. 5(a). At a gate voltage of  $-2$  to  $0$  V, the proton irradiation causes  $\sim 32\%$ – $10\%$  reduction of  $I_{ds,sat}$  for the pristine devices, whereas, the reduction of  $I_{ds,sat}$  for the micro-trenched devices is only  $\sim 13\%$ – $2\%$ . The relative increase of  $R_{ON}$  at a gate voltage of  $-2$  to  $0$  V for the pristine and micro-trenched

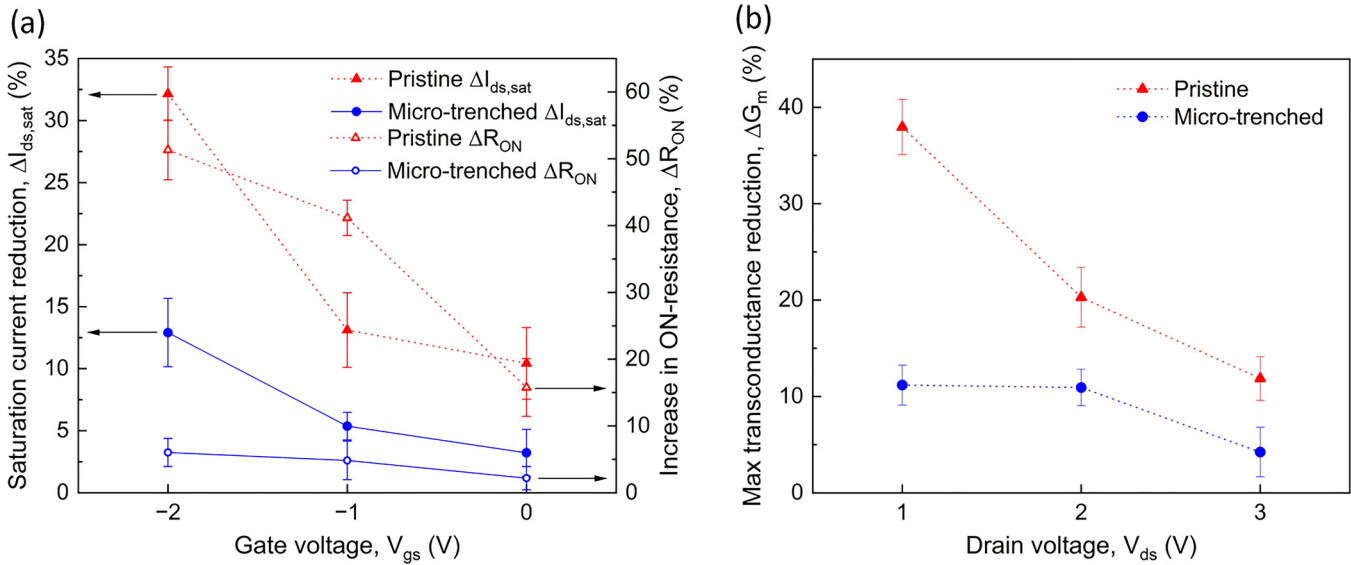


**FIG. 5.** Relative change of transport properties after proton irradiation showing (a) reduction of drain saturation current and increase of ON-resistance and (b) reduction of maximum transconductance.

devices is found to be  $\sim 51\%$ – $15\%$  and  $\sim 6\%$ – $2\%$ , respectively. Significant differences in maximum transconductance values are also observed after proton irradiation, as shown in Fig. 5(b). At a drain voltage of 1–3 V, the  $G_M$  values decrease by  $\sim 38\%$ – $10\%$  and  $\sim 11\%$ – $3\%$  for the pristine and micro-trenched devices, respectively.

The degraded transport properties of the devices after proton irradiation are attributed to the reduction of 2DEG sheet carrier density ( $n_s$ ) and mobility ( $\mu_n$ ). The  $n_s$  and  $\mu_n$  are estimated using the following equations from C–V measurements:<sup>65,66</sup>

$$n_s = \int_{V_{th}}^{V_{gs}} \frac{CdV}{Sq},$$

$$\mu_n = \frac{I_{ds}L_g}{qn_sW[V_{ds} - I_{ds}(R_D + R_S)]},$$

$$R_D = \frac{L_{gd}W}{qn_{s0}\mu_{n0}},$$

$$R_S = \frac{L_{gs}W}{qn_{s0}\mu_{n0}},$$

where  $S$  is the Schottky contact area,  $q$  is the electron charge,  $I_{ds}$  is the drain to source current at drain to source voltage of  $V_{ds} = 0.1$  V,  $W$  is the gate width,  $L_g$  is the gate length,  $L_{gd}$  is the gate to drain distance,  $L_{gs}$  is the gate to source voltage, and  $n_{s0}$  and  $\mu_{n0}$  are the electron density and mobility at zero gate bias, respectively. The effect of proton irradiation on the relative change of sheet carrier density ( $\Delta n_s$ ) and mobility ( $\Delta \mu_n$ ) is presented in Figs. 6(a) and 6(b),

respectively. The carrier density and mobility of both devices decrease after proton irradiation. This could be attributed to radiation induced defects such as gallium and nitrogen vacancies and interstitials. Dislocations and cracks can also be generated after proton irradiation. In addition, the strain in the GaN layer after irradiation for both devices is found to be higher compared to the pristine devices, as shown in Fig. 3(a). Higher tensile strain in the GaN layer could produce relaxation of strain in the AlGaN layer and AlGaN/GaN interface, which can nucleate defects and trap centers for electrons during operation reducing the mobility.<sup>67,68</sup> However, the degradation of the micro-trenched devices is far less severe compared to the pristine devices. The carrier density of the pristine and micro-trenched devices drops by  $\sim 15\%$ – $5\%$  and  $\sim 9\%$ – $3\%$ , respectively, for the gate voltage of  $-2$  to  $0$  V, which agrees with the results obtained by the Raman experiment, as shown in Fig. 3(b), by higher  $A_1$  (LO) phonon frequency of the micro-trenched devices compared to the pristine devices after irradiation. The reduction of mobility for the pristine devices is found to be  $\sim 48\%$ – $22\%$ , whereas the corresponding value for the micro-trenched devices is only  $\sim 30\%$ – $4\%$ . The displacement defects such as vacancies created by proton irradiation act as the charged trap centers within the bandgap. These trap centers capture the free carriers reducing the carrier concentration of the 2DEG.<sup>20,34</sup> The lattice defects also act as the scattering centers for electrons reducing the mobility.<sup>18,19,69</sup> In addition, proton irradiation is reported to increase the AlGaN/GaN interface roughness, which further increases the scattering of 2DEG electrons reducing the mobility of the device.<sup>13,24</sup> One important aspect of proton irradiation induced damage of both devices is that the gate voltage of the devices plays an important role in the degradation of transport properties, as can be seen in Figs. 5 and 6. The closer the gate voltage is to the

07 April 2024 10:49:38

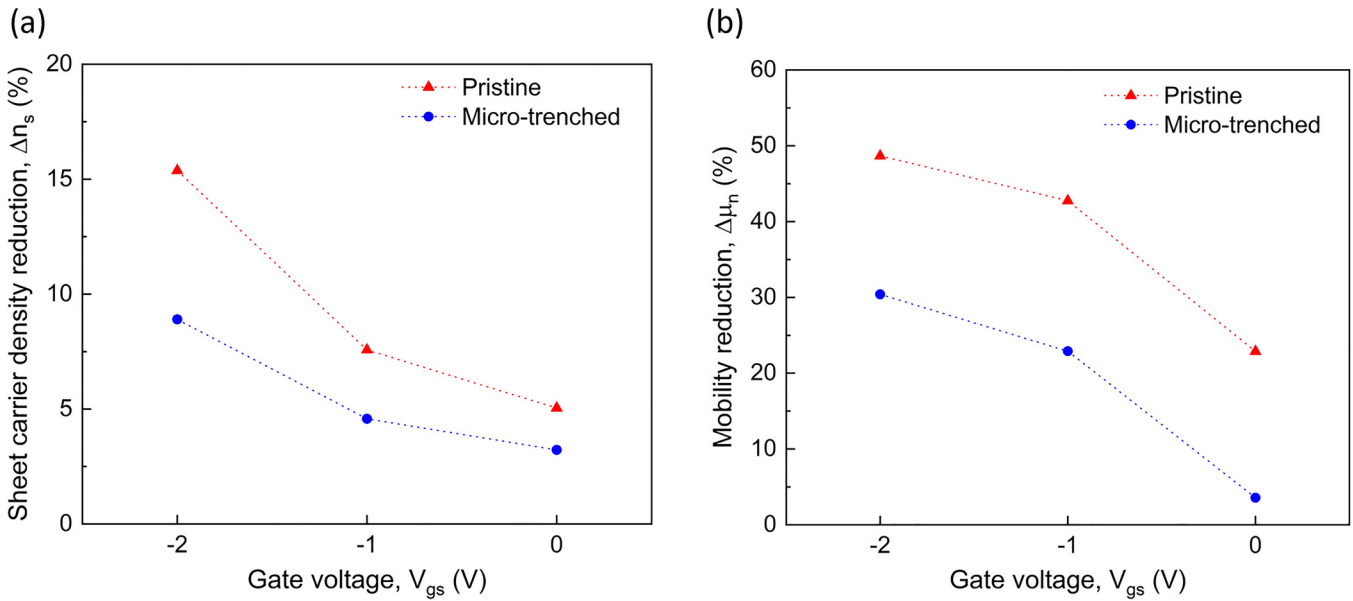


FIG. 6. Relative change of (a) sheet carrier density and (b) mobility of the pristine and micro-trenched devices after proton irradiation.

threshold voltage of the device, the higher the degradation, which might be due to the higher electric field associated with higher reverse bias. The higher electric field generates larger inverse-piezoelectric stress causing a strain relaxation in the AlGaIn and GaN layers and creates electrically active crystal defects.<sup>70</sup>

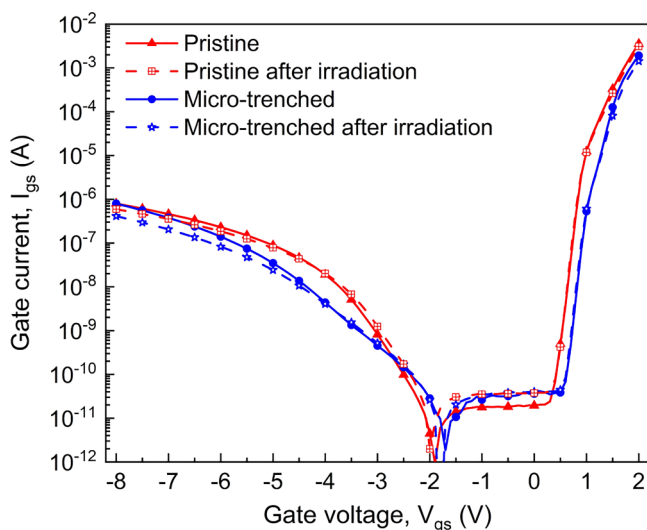


FIG. 7. Gate leakage current of the pristine and micro-trenched devices before and after proton irradiation.

The gate leakage currents of the pristine and micro-trenched devices before and after irradiation are shown in Fig. 7. After proton irradiation, the leakage current of both devices reduces slightly. The reduction of the gate leakage current could be due to the formation of the interfacial oxide layer, defects, and voids generated under the metal Schottky contact reducing the effective gate area.<sup>18,28,29</sup> However, the reduction of the gate leakage current of the pristine devices is relatively smaller compared to the micro-trenched devices, which may be associated with the higher strain relaxation in the AlGaIn barrier of the pristine devices compared to the micro-trenched devices leading to carrier tunneling and higher gate leakage.

Overall, the localized strain relaxed micro-trenched devices exhibit better radiation hardness compared to the pristine devices as demonstrated by a smaller reduction of drain saturation current, maximum transconductance, 2DEG carrier concentrations, and mobility along with smaller positive threshold voltage shifts and lower gate leakage current. Li *et al.*<sup>48</sup> reported that higher tensile strain in the GaN reduces its threshold displacement energy, which is inversely proportional to the defect density of the material. Relatively smaller tensile strain in the micro-trenched devices causes a smaller change in threshold displacement energy compared to the highly strained pristine device. As a result, the micro-trenched devices have smaller defect density after irradiation compared to the pristine counterparts, resulting in lower trap concentration and/or electrically active defects. In addition, localized strain relaxation of the micro-trenched devices is expected to induce smaller inverse-piezoelectric stress and thermoelastic stress along the channel,<sup>36</sup> which might reduce the scattering of electrons during operation leading to higher mobility, drain saturation

07 April 2024 10:49:38



current, and transconductance compared to the irradiated pristine devices.

## CONCLUSIONS

While the effect of strain and proton irradiation on AlGaIn/GaN HEMTs has been studied separately in the existing literature, their combined effects on the performance of GaN HEMTs have not been studied previously. Here, we investigate the proton irradiation induced degradation of AlGaIn/GaN HEMTs in the presence of localized strain relaxation, which is achieved by the micro-trenching technique. The 5 MeV proton irradiation at a fluence of  $5 \times 10^{14} \text{ cm}^{-2}$  causes additional strain in the GaN layer, which is initially under tensile strain. Although the local relaxation of tensile strain is found to reduce the drain output current and transconductance of the devices before irradiation, the post-irradiation properties are less susceptible to radiation damage compared to the pristine devices. The strain relieved devices show relatively smaller positive threshold voltage shifts after proton irradiation compared to the pristine devices. The degradation of the transport properties such as drain saturation current, maximum transconductance, sheet carrier density, and mobility of the strain relaxed micro-trenched devices is noticeably less severe compared to pristine devices. Relatively less susceptibility of proton irradiation damage for the localized strain relaxed devices compared to the pristine devices could be attributed to the smaller change in threshold displacement energy, smaller operation related stress such as inverse-piezoelectric stress and thermal stress leading to lower defect concentration and scattering of electrons during operation. Therefore, the relaxation of strain of AlGaIn/GaN HEMTs could be advantageous to alleviate the proton irradiation induced degradation to some extent.

## ACKNOWLEDGMENTS

We acknowledge the funding support from the U.S. National Science Foundation (ECCS No. 2015795). The study was partially supported by the Defense Threat Reduction Agency (DTRA) as part of the Interaction of Ionizing Radiation with Matter University Research Alliance (IIRM-URA) under Contract No. HDTRA1-20-2-0002. The work in Korea was supported by the K-Sensor Development Program (No. RS-2022-00154729), funded by the Ministry of Trade, Industry and Energy (MOTIE, Korea) and the National Research Foundation of Korea (No. 2020M3H4A3081799).

## AUTHOR DECLARATIONS

### Conflict of Interest

The authors have no conflicts to disclose.

### Author Contributions

**Nahid Sultan Al-Mamun:** Data curation (equal); Formal analysis (equal); Investigation (equal); Methodology (equal); Validation (equal); Visualization (equal); Writing – original draft (equal). **Joonyup Bae:** Formal analysis (equal); Investigation (equal); Methodology (equal). **Jihyun Kim:** Investigation (equal); Methodology (equal); Supervision (equal); Writing – review &

editing (equal). **Aman Haque:** Conceptualization (equal); Data curation (equal); Investigation (equal); Methodology (equal); Supervision (equal); Validation (equal); Writing – review & editing (equal). **Douglas E. Wolfe:** Conceptualization (equal); Funding acquisition (equal); Project administration (equal); Supervision (equal); Writing – review & editing (equal). **Fan Ren:** Conceptualization (equal); Investigation (equal); Methodology (equal); Validation (equal); Writing – review & editing (equal). **Stephen Pearton:** Conceptualization (equal); Funding acquisition (equal); Investigation (equal); Methodology (equal); Validation (equal); Writing – review & editing (equal).

## DATA AVAILABILITY

The data that support the findings of this study are available within the article.

## REFERENCES

- 1 E. A. Jones, F. F. Wang, and D. Costinett, "Review of commercial GaN power devices and GaN-based converter design challenges," *IEEE J. Emerging Sel. Top. Power Electron.* **4**(3), 707–719 (2016).
- 2 U. K. Mishra, L. Shen, T. E. Kazior, and Y. F. Wu, "GaN-based RF power devices and amplifiers," *Proc. IEEE* **96**(2), 287–305 (2008).
- 3 R. J. Trew, G. L. Bilbro, W. Kuang, Y. Liu, and H. Yin, "Microwave AlGaIn/GaN HFETs," *IEEE Microwave Mag.* **6**(1), 56–66 (2005).
- 4 S. J. Pearton, A. Aitkaliyeva, M. Xian, F. Ren, A. Khachatryan, A. Ildefonso, Z. Islam, M. A. Jafar Rasel, A. Haque, A. Y. Polyakov, and J. Kim, "Review—Radiation damage in wide and ultra-wide bandgap semiconductors," *ECS J. Solid State Sci. Technol.* **10**(5), 055008 (2021).
- 5 U. K. Mishra, P. Parikh, and W. Yi-Feng, "AlGaIn/GaN HEMTs—An overview of device operation and applications," *Proc. IEEE* **90**(6), 1022–1031 (2002).
- 6 J. A. del Alamo and J. Joh, "GaN HEMT reliability," *Microelectron. Reliab.* **49**(9), 1200–1206 (2009).
- 7 S. J. Pearton, Y.-S. Hwang, and F. Ren, "Radiation effects in GaN-based high electron mobility transistors," *J. Mater.* **67**(7), 1601–1611 (2015).
- 8 S. Pearton, X. Xia, F. Ren, M. A. J. Rasel, S. Stepanoff, N. Al-Mamun, A. Haque, and D. E. Wolfe, "Radiation damage in GaN/AlGaIn and SiC electronic and photonic devices," *J. Vac. Sci. Technol. B* **41**(3), 030802 (2023).
- 9 A. Ionascut-Nedelcescu, C. Carlone, A. Houdayer, H. J. V. Bardeleben, J. L. Cantin, and S. Raymond, "Radiation hardness of gallium nitride," *IEEE Trans. Nucl. Sci.* **49**(6), 2733–2738 (2002).
- 10 D. M. Fleetwood, E. X. Zhang, R. D. Schrimpf, and S. T. Pantelides, "Radiation effects in AlGaIn/GaN HEMTs," *IEEE Trans. Nucl. Sci.* **69**(5), 1105–1119 (2022).
- 11 S. J. Pearton, F. Ren, E. Patrick, M. E. Law, and A. Y. Polyakov, "Review—Ionizing radiation damage effects on GaN devices," *ECS J. Solid State Sci. Technol.* **5**(2), Q35 (2016).
- 12 B. N. Pushpakaran, A. S. Subburaj, and S. B. Bayne, "Commercial GaN-based power electronic systems: A review," *J. Electron. Mater.* **49**(11), 6247–6262 (2020).
- 13 S. Ahn, C. Dong, W. Zhu, B.-J. Kim, Y.-H. Hwang, F. Ren, S. J. Pearton, G. Yang, J. Kim, E. Patrick, B. Tracy, D. J. Smith, and I. I. Kravchenko, "Effect of proton irradiation energy on AlGaIn/GaN metal-oxide semiconductor high electron mobility transistors," *J. Vac. Sci. Technol. B* **33**(5), 051208 (2015).
- 14 T. J. Anderson, A. D. Koehler, J. D. Greenlee, B. D. Weaver, M. A. Mastro, J. K. Hite, C. R. Eddy, F. J. Kub, and K. D. Hobart, "Substrate-dependent effects on the response of AlGaIn/GaN HEMTs to 2-MeV proton irradiation," *IEEE Electron Device Lett.* **35**(8), 826–828 (2014).
- 15 B. Chatterjee, D. Shoemaker, Y. Song, T. Shi, H.-L. Huang, D. Keum, A. Krishnan, B. M. Foley, I. Jovanovic, J. Hwang, H. Kim, and S. Choi,

- "Cumulative impacts of proton irradiation on the self-heating of AlGaIn/GaN HEMTs," *ACS Appl. Electron. Mater.* **2**(4), 980–991 (2020).
- <sup>16</sup>J. D. Greenlee, P. Specht, T. J. Anderson, A. D. Koehler, B. D. Weaver, M. Luysberg, O. D. Dubon, F. J. Kub, T. R. Weatherford, and K. D. Hobart, "Degradation mechanisms of 2 MeV proton irradiated AlGaIn/GaN HEMTs," *Appl. Phys. Lett.* **107**(8), 083504 (2015).
- <sup>17</sup>H. Xinwen, A. P. Karmarkar, J. Bongim, D. M. Fleetwood, R. D. Schrimpf, R. D. Geil, R. A. Weller, B. D. White, M. Bataiev, L. J. Brillson, and U. K. Mishra, "Proton-irradiation effects on AlGaIn/AlN/GaN high electron mobility transistors," *IEEE Trans. Nucl. Sci.* **50**(6), 1791–1796 (2003).
- <sup>18</sup>M. P. Khanal, S. Upreti, V. Mirkhani, S. Wang, K. Yapabandara, E. Hassani, T. Isaacs-Smith, A. C. Ahyi, M. J. Zozack, T.-S. Oh, and M. Park, "Impact of 100 keV proton irradiation on electronic and optical properties of AlGaIn/GaN high electron mobility transistors (HEMTs)," *J. Appl. Phys.* **124**(21), 215702 (2018).
- <sup>19</sup>H. Y. Kim, J. Kim, S. P. Yun, K. R. Kim, T. J. Anderson, F. Ren, and S. J. Pearton, "AlGaIn/GaN high electron mobility transistors irradiated with 17 MeV protons," *J. Electrochem. Soc.* **155**(7), H513 (2008).
- <sup>20</sup>H. Y. Kim, J. Kim, L. Liu, C. F. Lo, F. Ren, and S. J. Pearton, "Effects of proton irradiation energies on degradation of AlGaIn/GaN high electron mobility transistors," *J. Vac. Sci. Technol. B* **30**(1), 012202 (2012).
- <sup>21</sup>B. Luo, J. W. Johnson, F. Ren, K. K. Allums, C. R. Abernathy, S. J. Pearton, R. Dwivedi, T. N. Fogarty, R. Wilkins, A. M. Dabiran, A. M. Wowchack, C. J. Polley, P. P. Chow, and A. G. Baca, "Dc and rf performance of proton-irradiated AlGaIn/GaN high electron mobility transistors," *Appl. Phys. Lett.* **79**(14), 2196–2198 (2001).
- <sup>22</sup>L. Lv, J. G. Ma, Y. R. Cao, J. C. Zhang, W. Zhang, L. Li, S. R. Xu, X. H. Ma, X. T. Ren, and Y. Hao, "Study of proton irradiation effects on AlGaIn/GaN high electron mobility transistors," *Microelectron. Reliab.* **51**(12), 2168–2172 (2011).
- <sup>23</sup>C. H. Sun, C. Peng, Z. G. Zhang, J. B. Wang, S. Z. Yue, H. Zhang, Z. W. Chen, X. P. Ou Yang, Z. F. Lei, and X. L. Zhong, "Mechanism of reverse gate leakage current reduction in AlGaIn/GaN high-electron-mobility-transistor after 3-MeV proton irradiation," *Appl. Phys. Lett.* **121**(7), 072109 (2022).
- <sup>24</sup>B. D. White, M. Bataiev, S. H. Goss, X. Hu, A. Karmarkar, D. M. Fleetwood, R. D. Schrimpf, W. J. Schaff, and L. J. Brillson, "Electrical, spectral, and chemical properties of 1.8 MeV proton irradiated AlGaIn/GaN HEMT structures as a function of proton fluence," *IEEE Trans. Nucl. Sci.* **50**(6), 1934–1941 (2003).
- <sup>25</sup>S. Yue, Z. Lei, C. Peng, X. Zhong, J. Wang, Z. Zhang, Y. En, Y. Wang, and L. Hu, "High-fluence proton-induced degradation on AlGaIn/GaN high-electron-mobility transistors," *IEEE Trans. Nucl. Sci.* **67**(7), 1339–1344 (2020).
- <sup>26</sup>H. Xinwen, B. K. Choi, H. J. Barnaby, D. M. Fleetwood, R. D. Schrimpf, L. Sungchul, S. Shojah-Ardalan, R. Wilkins, U. K. Mishra, and R. W. Dettmer, "The energy dependence of proton-induced degradation in AlGaIn/GaN high electron mobility transistors," *IEEE Trans. Nucl. Sci.* **51**(2), 293–297 (2004).
- <sup>27</sup>B. Luo, J. W. Johnson, F. Ren, K. K. Allums, C. R. Abernathy, S. J. Pearton, R. Dwivedi, T. N. Fogarty, R. Wilkins, A. M. Dabiran, A. M. Wowchack, C. J. Polley, P. P. Chow, and A. G. Baca, "High-energy proton irradiation effects on AlGaIn/GaN high-electron mobility transistors," *J. Electron. Mater.* **31**(5), 437–441 (2002).
- <sup>28</sup>D. S. Kim, J. H. Lee, J. G. Kim, Y. J. Yoon, J. S. Lee, and J. H. Lee, "Anomalous DC characteristics of AlGaIn/GaN HEMTs depending on proton irradiation energies," *ECS J. Solid State Sci. Technol.* **9**(6), 065005 (2020).
- <sup>29</sup>A. D. Koehler, P. Specht, T. J. Anderson, B. D. Weaver, J. D. Greenlee, M. J. Tadjer, M. Porter, M. Wade, O. C. Dubon, K. D. Hobart, T. R. Weatherford, and F. J. Kub, "Proton radiation-induced void formation in Ni/Au-gated AlGaIn/GaN HEMTs," *IEEE Electron Device Lett.* **35**(12), 1194–1196 (2014).
- <sup>30</sup>A. D. Koehler, T. J. Anderson, M. J. Tadjer, B. D. Weaver, J. D. Greenlee, D. I. Shahin, K. D. Hobart, and F. J. Kub, "Impact of surface passivation on the dynamic ON-resistance of proton-irradiated AlGaIn/GaN HEMTs," *IEEE Electron Device Lett.* **37**(5), 545–548 (2016).
- <sup>31</sup>J. C. Gallagher, T. J. Anderson, A. D. Koehler, N. A. Mahadik, A. Nath, B. D. Weaver, K. D. Hobart, and F. J. Kub, "Effect of surface passivation and substrate on proton irradiated AlGaIn/GaN HEMT transport properties," *ECS J. Solid State Sci. Technol.* **6**(11), S3060 (2017).
- <sup>32</sup>J. H. Lee, D. S. Kim, J. G. Kim, W. H. Ahn, Y. Bae, and J. H. Lee, "Effect of gate dielectrics on characteristics of high-energy proton-irradiated AlGaIn/GaN MISHEMTs," *Radiat. Phys. Chem.* **184**, 109473 (2021).
- <sup>33</sup>A. P. Karmarkar, J. Bongim, D. M. Fleetwood, R. D. Schrimpf, R. A. Weller, B. D. White, L. J. Brillson, and U. K. Mishra, "Proton irradiation effects on GaN-based high electron-mobility transistors with Si-doped Al/sub x/Ga/sub 1-x/N and thick GaN cap layers," *IEEE Trans. Nucl. Sci.* **51**(6), 3801–3806 (2004).
- <sup>34</sup>D. S. Kim, J. H. Lee, and S. Yeo, "Proton irradiation effects on AlGaIn/GaN HEMTs with different isolation methods," *IEEE Trans. Nucl. Sci.* **65**(1), 579–582 (2018).
- <sup>35</sup>H. J. Park, C. Park, S. Yeo, S. W. Kang, M. Mastro, O. Kryliouk, and T. J. Anderson, "Epitaxial strain energy measurements of GaN on sapphire by Raman spectroscopy," *Phys. Status Solidi C* **2**(7), 2446–2449 (2005).
- <sup>36</sup>T. Beechem, A. Christensen, D. S. Green, and S. Graham, "Assessment of stress contributions in GaN high electron mobility transistors of differing substrates using Raman spectroscopy," *J. Appl. Phys.* **106**(11), 114509 (2009).
- <sup>37</sup>B. S. Kang, S. Kim, J. Kim, F. Ren, K. Baik, S. J. Pearton, B. P. Gila, C. R. Abernathy, C. C. Pan, G. T. Chen, J. I. Chyi, V. Chandrasekaran, M. Sheplak, T. Nishida, and S. N. G. Chu, "Effect of external strain on the conductivity of AlGaIn/GaN high-electron-mobility transistors," *Appl. Phys. Lett.* **83**(23), 4845–4847 (2003).
- <sup>38</sup>H.-L. Kao, H.-C. Chiu, S.-H. Chuang, and H. H. Hsu, "AlGaIn/GaN high-electron-mobility transistors on a silicon substrate under uniaxial tensile strain," *ECS J. Solid State Sci. Technol.* **9**(4), 045017 (2020).
- <sup>39</sup>C. T. Chang, S. K. Hsiao, E. Y. Chang, C. Y. Lu, J. C. Huang, and C. T. Lee, "Changes of electrical characteristics for AlGaIn/GaN HEMTs under uniaxial tensile strain," *IEEE Electron Device Lett.* **30**(3), 213–215 (2009).
- <sup>40</sup>K. Liu, H. Zhu, S. Feng, L. Shi, Y. Zhang, and C. Guo, "The effect of external strain on the electrical characteristics of AlGaIn/GaN HEMTs," *Microelectron. Reliab.* **55**(6), 886–889 (2015).
- <sup>41</sup>E. Cho, A. Mogilatenko, F. Brunner, E. Richter, and M. Weyers, "Impact of AlN nucleation layer on strain in GaN grown on 4H-SiC substrates," *J. Cryst. Growth* **371**, 45–49 (2013).
- <sup>42</sup>S. Shervin, S. H. Kim, M. Asadirad, S. Ravipati, K. H. Lee, K. Bulashevich, and J. H. Ryoo, "Strain-effect transistors: Theoretical study on the effects of external strain on III-nitride high-electron-mobility transistors on flexible substrates," *Appl. Phys. Lett.* **107**(19), 193504 (2015).
- <sup>43</sup>M. Azize and T. Palacios, "Effect of substrate-induced strain in the transport properties of AlGaIn/GaN heterostructures," *J. Appl. Phys.* **108**(2), 023707 (2010).
- <sup>44</sup>H. Zhu, X. Meng, X. Zheng, Y. Yang, S. Feng, Y. Zhang, and C. Guo, "Effect of substrate thinning on the electronic transport characteristics of AlGaIn/GaN HEMTs," *Solid State Electron.* **145**, 40–45 (2018).
- <sup>45</sup>M. Broas, A. Graff, M. Simon-Najasek, D. Poppitz, F. Altmann, H. Jung, and H. Blanck, "Correlation of gate leakage and local strain distribution in GaN/AlGaIn HEMT structures," *Microelectron. Reliab.* **64**, 541–546 (2016).
- <sup>46</sup>M. Mikulics, P. Kordoš, D. Gregušová, Š. Gaži, J. Novák, Z. Sofer, J. Mayer, and H. Hardtgen, "Local increase in compressive strain (GaN) in gate recessed AlGaIn/GaN MISHFET structures induced by an amorphous AlN dielectric layer," *Semicond. Sci. Technol.* **36**(9), 095040 (2021).
- <sup>47</sup>M. A. J. Rasel, S. Stepanoff, A. Haque, D. E. Wolfe, F. Ren, and S. Pearton, "Nanoscale stress localization effects on the radiation susceptibility of GaN high-mobility transistors," *Phys. Status Solidi Rapid Res. Lett.* **16**(8), 2200171 (2022).
- <sup>48</sup>Q. Li, H. Lou, and L. Zhu, "Strain effect on the performance of proton-irradiated GaN-based HEMT," *Appl. Phys. A* **129**(5), 374 (2023).
- <sup>49</sup>A. M. Korsunsky, M. Sebastiani, and E. Bemporad, "Focused ion beam ring drilling for residual stress evaluation," *Mater. Lett.* **63**(22), 1961–1963 (2009).
- <sup>50</sup>M. Sebastiani, C. Eberl, E. Bemporad, A. M. Korsunsky, W. D. Nix, and F. Carassiti, "Focused ion beam four-slot milling for Poisson's ratio and residual stress evaluation at the micron scale," *Surf. Coat. Technol.* **251**, 151–161 (2014).

- <sup>51</sup>N. S. Al-Mamun, M. Wetherington, D. E. Wolfe, A. Haque, F. Ren, and S. Pearton, "Local strain modification effects on global properties of AlGaIn/GaN high electron mobility transistors," *Microelectron. Eng.* **262**, 111836 (2022).
- <sup>52</sup>J. F. Ziegler and J. P. Biersack, "The stopping and range of ions in matter," in *Treatise on Heavy-Ion Science: Volume 6: Astrophysics, Chemistry, and Condensed Matter*, edited by D. A. Bromley (Springer US, Boston, MA, 1985), pp. 93–129.
- <sup>53</sup>J. F. Ziegler, M. D. Ziegler, and J. P. Biersack, "SRIM—The stopping and range of ions in matter (2010)," *Nucl. Instrum. Methods Phys. Res. Sec. B* **268**(11), 1818–1823 (2010).
- <sup>54</sup>Y. S. Puzyrev, T. Roy, E. X. Zhang, D. M. Fleetwood, R. D. Schrimpf, and S. T. Pantelides, "Radiation-induced defect evolution and electrical degradation of AlGaIn/GaN high-electron-mobility transistors," *IEEE Trans. Nucl. Sci.* **58**(6), 2918–2924 (2011).
- <sup>55</sup>A. Stocco, S. Gerardin, D. Bisi, S. Dalcanale, F. Rampazzo, M. Meneghini, G. Meneghesso, J. Grünenpütt, B. Lambert, H. Blanck, and E. Zanoni, "Proton induced trapping effect on space compatible GaN HEMTs," *Microelectron. Reliab.* **54**(9), 2213–2216 (2014).
- <sup>56</sup>A. Kalavagunta, A. Touboul, L. Shen, R. D. Schrimpf, R. A. Reed, D. M. Fleetwood, R. K. Jain, and U. K. Mishra, "Electrostatic mechanisms responsible for device degradation in proton irradiated AlGaIn/AlN/GaN HEMTs," *IEEE Trans. Nucl. Sci.* **55**(4), 2106–2112 (2008).
- <sup>57</sup>T. Beechem, A. Christensen, S. Graham, and D. Green, "Micro-Raman thermometry in the presence of complex stresses in GaN devices," *J. Appl. Phys.* **103**(12), 124501 (2008).
- <sup>58</sup>S. Tripathy, S. J. Chua, P. Chen, and Z. L. Miao, "Micro-Raman investigation of strain in GaN and Al<sub>x</sub>Ga<sub>1-x</sub>N/GaN heterostructures grown on Si(111)," *J. Appl. Phys.* **92**(7), 3503–3510 (2002).
- <sup>59</sup>A. Abderrahmane, S. Koide, H. Okada, H. Takahashi, S. Sato, T. Ohshima, and A. Sandhu, "Effect of proton irradiation on AlGaIn/GaN micro-Hall sensors," *Appl. Phys. Lett.* **102**(19), 193510 (2013).
- <sup>60</sup>H. Y. Kim, J. A. Freitas, and J. Kim, "Penetration effects of high-energy protons in GaN: A micro-Raman spectroscopy study," *Electrochem. Solid State Lett.* **14**(1), H5 (2011).
- <sup>61</sup>L. Lv, X. Ma, J. Zhang, Z. Bi, L. Liu, H. Shan, and Y. Hao, "Proton irradiation effects on AlGaIn/AlN/GaN heterojunctions," *IEEE Trans. Nucl. Sci.* **62**(1), 300–305 (2015).
- <sup>62</sup>R. X. Wang, S. J. Xu, S. Fung, C. D. Beling, K. Wang, S. Li, Z. F. Wei, T. J. Zhou, J. D. Zhang, Y. Huang, and M. Gong, "Micro-Raman and photoluminescence studies of neutron-irradiated gallium nitride epilayers," *Appl. Phys. Lett.* **87**(3), 031906 (2005).
- <sup>63</sup>H. Y. Kim, J. A. Freitas, and J. Kim, "Probing proton irradiation effects in GaN by micro-Raman spectroscopy," *Europhys. Lett.* **96**(2), 26004 (2011).
- <sup>64</sup>T. Roy, E. X. Zhang, Y. S. Puzyrev, D. M. Fleetwood, R. D. Schrimpf, B. K. Choi, A. B. Hmelo, and S. T. Pantelides, "Process dependence of proton-induced degradation in GaN HEMTs," *IEEE Trans. Nucl. Sci.* **57**(6), 3060–3065 (2010).
- <sup>65</sup>J. Zhao, Z. Lin, T. D. Corrigan, Z. Wang, Z. You, and Z. Wang, "Electron mobility related to scattering caused by the strain variation of AlGaIn barrier layer in strained AlGaIn/GaN heterostructures," *Appl. Phys. Lett.* **91**(17), 173507 (2007).
- <sup>66</sup>Y. J. Lv, X. B. Song, Y. G. Wang, Y. L. Fang, and Z. H. Feng, "Influence of surface passivation on AlN barrier stress and scattering mechanism in ultra-thin AlN/GaN heterostructure field-effect transistors," *Nanoscale Res. Lett.* **11**(1), 373 (2016).
- <sup>67</sup>H. V. Stanchu, A. V. Kuchuk, Y. I. Mazur, C. Li, P. M. Lytvyn, M. Schmidbauer, Y. Maidaniuk, M. Benamara, M. E. Ware, Z. M. Wang, and G. J. Salamo, "Local strain and crystalline defects in GaN/AlGaIn/GaN(0001) heterostructures induced by compositionally graded AlGaIn buried layers," *Cryst. Growth Des.* **19**(1), 200–210 (2019).
- <sup>68</sup>E. W. Blanton, G. Siegel, T. A. Prusnick, N. R. Glavin, and M. Snure, "Strain-induced changes in AlGaIn/GaN two-dimensional electron gas structures with low surface state densities," *Appl. Phys. Lett.* **113**(26), 263503 (2018).
- <sup>69</sup>C. F. Lo, C. Y. Chang, B. H. Chu, H. Y. Kim, J. Kim, D. A. Cullen, L. Zhou, D. J. Smith, S. J. Pearton, A. Dabiran, B. Cui, P. P. Chow, S. Jang, and F. Ren, "Proton irradiation effects on AlN/GaN high electron mobility transistors," *J. Vac. Sci. Technol. B* **28**(5), L47–L51 (2010).
- <sup>70</sup>M. Meneghini, A. Stocco, M. Bertin, D. Marcon, A. Chini, G. Meneghesso, and E. Zanoni, "Time-dependent degradation of AlGaIn/GaN high electron mobility transistors under reverse bias," *Appl. Phys. Lett.* **100**(3), 033505 (2012).